Original Article

Institution of MECHANICAL ENGINEERS
Journal of PROCESS MECHANICAL ENGINEERING

Proc IMechE Part E:
J Process Mechanical Engineering
0(0) 1–9

DOI: 10.1177/0954408912472172
uk.sagepub.com/jpme
SAGE

Numerical simulation of flow velocity profiles along a stepped spillway

Duangrudee Kositgittiwong[1], Chaiyuth Chinnarasri[1] and Pierre Y Julien[2]

Abstract

The velocity profiles on stepped spillways are analyzed using computational fluid dynamics simulations and large-scale laboratory experiments. Five different turbulence models are considered in the analysis: the Standard k-ε, the Realizable k-ε, the Renormalization group k-ε, the Standard k-ω and the Shear stress transport k-ω model. The computational fluid dynamics simulation results are compared with laboratory measurements from a large-scale physical model with flow velocities up to 15 m/s. It is indicated that the numerical model involving any of these turbulence models can satisfactorily simulate the velocity profiles. All five turbulence models performed satisfactorily well on large-scale stepped spillways. The k-ω models may be slightly better suited in the lower region, while the realizable k-ε model provided slightly better results in the upper part of the velocity profile. A power law with $n = 5.09$ also provides a useful first approximation with a limitation of the flow along stepped spillway with the Reynolds number of $1.68 \times 10^6 \leqslant Re \leqslant 7.21 \times 10^6$.

Keywords

Velocity profiles, computational fluid dynamics simulations, k-ε turbulence model, k-ω turbulence model, stepped spillway

Date received: 4 October 2012; accepted: 30 November 2012

Introduction

The construction of stepped spillways has recently become popular in many countries. Stepped spillways increase the rate of energy dissipation compared with traditional, smooth-surface spillways that require energy dissipation structures at their downstream end. The rate of energy dissipation on each step is greatly increased and ultimately.[1,2]

The flow regime on a stepped spillway is classified into three types: nappe flow, transition and skimming flow.[3–5] In nappe flow, usually found on large steps or at low discharges, a free-falling jet impacts from step to step with a fully aerated nappe cavity.[6] Skimming flows occur on small steps or at high discharges.[1,3] The air pocket along the vertical face of each step disappears in skimming flows. The transition occurs at discharges higher than the maximum required for nappe flow but lower than for the onset of skimming flow. The flow on each step generates a large horizontal vortex that recirculates water with or without air entrainment, whilst the water surface is wavy. For practical engineering purposes, skimming flows are more relevant than nappe flows.

At the upstream end of skimming flows over stepped spillways, the water surface is rather smooth without air entrainment. The boundary layer thickness is less than the flow depth and this zone is called the 'non-aerated zone'. The boundary layer develops and reaches the flow depth after a few steps at a location called the inception point. Downstream of the inception point, flow is rapidly aerated. The free surface becomes wavy with significant air entrainment in this zone, called the 'aerated zone'.[7–9] At each section of the aerated zone, the flow depth can be divided into at least two regions. The lower region beneath the pseudo-bottom consists of water containing individual air bubbles distributed throughout the flow and exchanged with the upper region. The upper region, above the pseudo-bottom, contains flow along the spillway. A wavy water surface in which air is trapped by waves is found.[1,7,10,11]

[1]Water Resources Engineering & Management Research Center (WAREE), King Mongkut's University of Technology Thonburi, Bangkok, Thailand
[2]Department of Civil and Environmental Engineering, Colorado State University, Colorado, USA

Corresponding author:
Chaiyuth Chinnarasri, Water Resources Engineering & Management Research Center (WAREE), King Mongkut's University of Technology Thonburi, Bangkok 10140, Thailand.
Email: chaiyuth.chi@kmutt.ac.th

Many scaled-down physical model studies investigating flow over stepped spillways have been carried out in the past. However, such modelling investigations are still vague due to the complexity of the flow.

Numerical modelling of spillways has become attractive due to increasing computer performance and advances in computational fluid dynamics (CFD). However, appropriate numerical models are needed to simulate the complexity of aerated flows on stepped spillways. One of the CFD model studies in the spillway is from Kim et al.[12] The FLOW-3d model was used with the initial design plan of the Karian dam in Indonesia. The results showed that the flow in the approach channel was unstable. A revised plan was formulated and the appropriate amended design was examined using numerical modeling.

The study by Chen et al.[13] indicates that the use of numerical simulations involving turbulence modelling is an efficient way to investigate the complexities of stepped spillway overflow. They used the k-ε turbulence model and the volume of fluid (VOF) method. The physical model of a 13-step spillway was set up to collect data for comparison with the numerical model. The first five step heights were 2, 2.4, 3, 4 and 5 cm. A uniform step height of 6 cm continued from step number 6 down to the toe. Cheng et al.[9] used the results from this physical model again. The renormalization group k-ε model (RNG k-ε) was chosen and their numerical results successfully reproduced the flow over the stepped spillway of the physical model. The results were helpful for understanding the rates of energy dissipation.

Qian et al.[14] simulated a 40-step spillway where the first 37 steps had a uniform 5 cm height and the last 3 steps varied in height, using four turbulence models: the realizable k-ε (Rl k-ε), the shear stress transport k-ω (SST k-ω), the v^2-f model and the large eddy simulation (LES). They concluded that Rl k-ε was the most efficient turbulence model for the simulation of flow over stepped spillways. Tongkratoke et al.[15] used other turbulence models: a linear, the LES and the non-linear model of Craft et al.[16] They modified the non-linear model to simulate the stepped spillways from Chanson and Toombes[10] and Boes and Hager.[7] The Rl k-ε showed the most satisfactory results amongst the linear turbulence models. The modified non-linear model also showed higher accuracy than other non-linear models.

One of the main questions in modelling stepped spillways is whether the physical and numerical models calibrated on small-scale physical models, can properly replicate the flow properties on large stepped spillways at the near-prototype scale. Listed in Table 1 is a summary of the geometries of the various model-scale studies and corresponding turbulence models. The physical model carried out at Colorado State University[17] has the largest step height. The flow discharge up to 3.3 m^3/s corresponds to Reynolds numbers ranging from $1.68 \times 10^6 \leqslant Re \leqslant 7.21 \times 10^6$. The physical model used in the present study is thus, the largest in size or near-prototype size, ever simulated by a numerical model. The results from the present study will be shown that the numerical model can be appropriately used to simulate the flow velocity profiles on the large stepped spillways at the near-prototype scale with just a small error. Then, in order to design the stepped spillway, this kind of the numerical model can be confidently used without any

Table 1. Geometry of previous and present studies of numerical models on stepped spillways.

Reference	Physical model studies	Discharge Q (m^3/s)	Specific discharge q $m^3/s/m$)	Geometry			Maximum roughness $K_s = h\cos\theta$ (m)	Number of steps N
				Slope θ (degree)	Spillway height H (m)	Step height h (m)		
Chen et al.[13]	Chen et al.[13]	0.0667	0.0200	53.1	0.79	0.02–0.06	0.04	13
Cheng et al.[9]	Chen et al.[13]	0.1000	0.0300	53.1	0.83	0.02–0.06	0.04	13
Qian et al.[14]	Amador[11]	0.1100	0.0800	51.3	2.00	0.0500	0.03	40
Tongkratoke et al.[15]	Boes and Hager[7]	0.0466	0.0233	30.0	2.85	0.0231	0.02	N/A
		0.1319	0.0660	30.0	2.85	0.0462	0.04	N/A
		0.3732	0.1866	30.0	2.85	0.0924	0.08	N/A
		0.0656	0.0328	50.0	4.36	0.0311	0.02	N/A
		0.3409	0.1705	50.0	4.36	0.0933	0.06	N/A
	Chanson and Toombes[10]	0.0580	0.0580	21.8	1.00	0.1000	0.10	9
		0.1140	0.1140	21.8	1.00	0.1000	0.10	9
Present study	Ward[17]	0.4645	0.5663	26.6	15.24	0.61	0.55	25
		0.9291	1.1327	26.6	15.24	0.61	0.55	25
		1.3935	1.6990	26.6	15.24	0.61	0.55	25
		1.8580	2.2653	26.6	15.24	0.61	0.55	25
		2.3226	2.8317	26.6	15.24	0.61	0.55	25
		2.6942	3.2848	26.6	15.24	0.61	0.55	25

N/A: not available.

need of physical model or without time consuming due to the complexity of the flow.

The aim of this study is to establish which turbulence model is appropriate for the simulation of skimming flow over stepped spillways and to predict the flow velocity with smallest deviation in terms of the root mean square error (RMSE). The simulation results are discussed by comparing the computed and measured velocity profiles at several locations along the 30 m spillway. A modified exponent of the velocity profile approximations using the power law is also presented.

Numerical simulation

The CFD code Fluent (Fluent Inc.) is used to solve the governing equations using the finite volume method (FVM). The CFD code simulates the near-prototype stepped spillway at Colorado State University (CSU). The overall length of the 25-step spillway sketched in Figure 1 is $L = 34.09$ m. The flume is 1.22 m wide and 2.13 m deep on a 2 H:1V slope, or $\theta = 26.6^\circ$. The total drop height H, is 15.24 m over horizontal length L_H, of 30.48 m. The discharge flow rates tested were 0.57, 1.13, 1.70, 2.27, 2.83 and 3.28 m^3/s. This study focused on the four largest discharges, which corresponds to unit discharges as high as 2.69 m^2/s. The velocity profiles were measured at five locations; labelled as A, B, C, D and E, at the tip of step numbers $i = 4$, 8, 12, 16 and 20, respectively. These correspond to the relative horizontal distance, il/L_H, of 0.16, 0.31, 0.47, 0.63 and 0.79. Velocity measurements were made perpendicular to the pseudo-bottom, which is shown in Figure 1 and defined by a straight line connecting the edges of each step.[18] To measure the velocity along the centerline of the spillway, Ward[17] used a back flushing pitot static tube.

The VOF method was used as a multiphase model. Hirt and Nichols[19] developed it for applications where two or more phases are not interpenetrating. In the present study, the velocity is measured from the pseudo-bottom to the free surface, which is located at air concentration of 90%, V_{90}. Therefore, the position of the free surface or the interface between air and water is of interest. The VOF solves equation (1) for tracking the free surface throughout the domain by using the geometric reconstruction scheme

$$\frac{\partial \alpha_w}{\partial t} + u_i \frac{\partial \alpha_w}{\partial x_i} = 0 \tag{1}$$

where α_w and α_a are volume fraction of water and air, respectively. A value of α_w equal to 0 and 1 means there is full air and water, respectively.

A set of continuity and momentum equations is

$$\frac{\partial \rho}{\partial t} + \frac{\partial \rho u_i}{\partial x_i} = 0 \tag{2}$$

$$\frac{\partial \rho u_i}{\partial t} + \frac{\partial \rho u_i u_j}{\partial x_j} = -\frac{\partial P}{\partial x_i} + \frac{\partial}{\partial x_j}(\mu + \mu_t)\left(\frac{\partial u_i}{\partial x_j} + \frac{\partial u_j}{\partial x_i}\right) \tag{3}$$

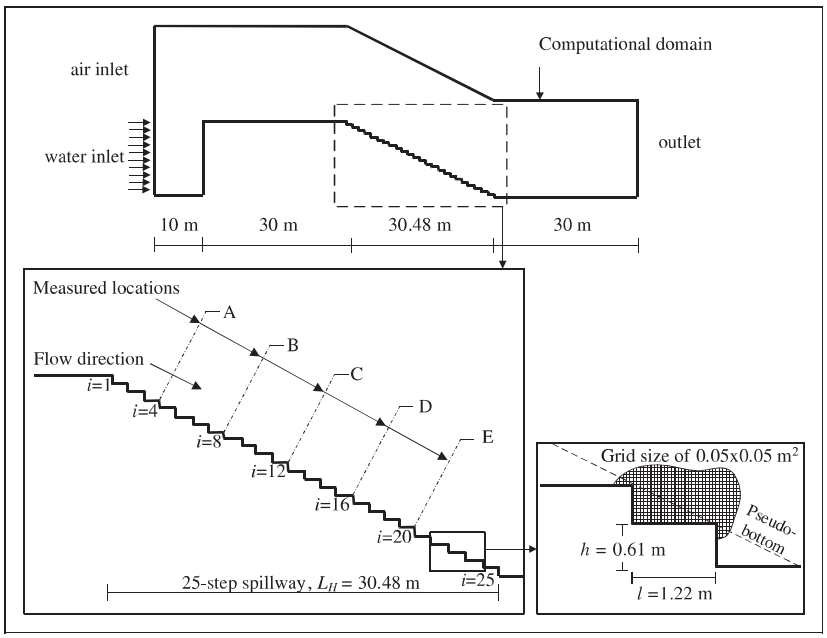

Figure 1. Schematic diagram of the CSU stepped spillway experiments.
CSU: Colorado State University.

where ρ is the cell density (kg/m^3), t, time (s), u_i and u_j, velocity (m/s) in x_i- and x_j- direction, respectively, P, pressure (N/m^2), μ, molecular dynamic viscosity (kg/m-s), μ_t, turbulent dynamic viscosity (kg/m-s).

The primary features of interest in a turbulent flow over a stepped spillway are: (1) the flow recirculation zone behind every step and (2) the turbulent free surface with a highly fluctuating velocity field downstream of the inception point where the inception point was found after 12 steps or more than that, depending on the inlet discharge. The turbulent motion of water and air near the surface causes significant difficulties in collecting velocity profiles up to the free surface. Therefore, the numerical simulations can be helpful in simulating the entire flow field. However, for flows over stepped spillways, the turbulence terms in the momentum equations play a dominant role in the definition of surface friction and resistance to flow. Thus, without using any turbulence model, the velocity distribution tends to become rather uniform. Typically, the pressure gradient counterbalances the velocity gradient, which leads to improper flow simulations over stepped spillways.[20] Turbulence models can represent and solve the approximation of the Reynolds stresses in terms of μ_t or the turbulent dynamic viscosity in the Reynolds-averaged Navier–Stokes equations (equation (3)).

The outer limit of the computational domain is shown in Figure 1. It was the real size of the near-prototype physical model. The boundary conditions include a uniform inflow velocity into the spillway inlet. The air boundary or free surface along the entire domain is set at the atmospheric pressure condition. The outflow is set as a pressure outlet and the walls considered impervious surfaces. The experimental flume was assumed to be sufficiently wide to allow two-dimensional simulation with a structured grid size of $0.05 \times 0.05\,\text{m}^2$. The grid convergence index (GCI) suggested by Roache[21] already assessed this grid size.

The GCI is a measure of the percentage the computed value is away from the numerical value, compared between two grid sizes. In the present study, three structured grid sizes of 0.035×0.035, 0.05×0.05 and $0.10 \times 0.10\,\text{m}^2$ were investigated for a comparison of the results. Then, the study of $\text{GCI}_{0.05,0.035}$, which is the comparison between the grid size of 0.035×0.035 and $0.05 \times 0.05\,\text{m}^2$ and $\text{GCI}_{0.10,0.05}$, which is the comparison between the grid size of 0.05×0.05 and $0.10 \times 0.10\,\text{m}^2$, are calculated. It shows $\text{GCI}_{0.05,0.035}$ and $\text{GCI}_{0.10,0.05}$ of less than 5 and 20%, respectively. From the comparison of numerical results at all locations, $\text{GCI}_{0.05,0.035}$ cannot be noticably seen whereas $\text{GCI}_{0.10,0.05}$ can be clearly seen or much higher than $\text{GCI}_{0.05,0.035}$. It means grid sizes of 0.035×0.035 and $0.05 \times 0.05\,\text{m}^2$ provided similar results, such that the $0.05 \times 0.05\,\text{m}^2$ grid was selected because of the significantly reduced time and resources required for the simulation.

Turbulence models

Among the linear turbulence models, the widely used two-equation model is based on: (1) the turbulent kinetic energy equation k and (2) the turbulent eddy dissipation ε, or the turbulent frequency ω. Five different turbulence models were chosen in the present study to simulate the flow over stepped spillways: the Standard k-ε, the Realizable k-ε, the Renormalization group k-ε, the Standard k-ω and the Shear stress transport k-ω model.

Standard k-ε model (St k-ε)

Launder and Spalding[22] developed the St k-ε model. The assumption is that the flow is fully turbulent and the effects of molecular viscosity are negligible. Therefore, the standard k-ε model is valid only for fully turbulent flows. The default values of the model constants have been determined from experiments with air and water for fundamental turbulent shear flows, including homogeneous shear flows and decaying isotropic grid turbulence. They have been found to work fairly well for a wide range of wall-bounded and free shear flows. It is a semi-empirical model based on the transport equations for k and ε, equations (4) and (5), respectively

$$\frac{\partial}{\partial t}(\rho k) + \frac{\partial}{\partial x_j}\left(\rho k u_j\right) = \frac{\partial}{\partial x_j}\left[\left(\mu + \frac{\mu_t}{\sigma_k}\right)\frac{\partial k}{\partial x_j}\right] + G_k + G_b - \rho\varepsilon - Y_M + S_k \quad (4)$$

$$\frac{\partial}{\partial t}(\rho \varepsilon) + \frac{\partial}{\partial x_i}(\rho \varepsilon u_i) = \frac{\partial}{\partial x_j}\left[\left(\mu + \frac{\mu_t}{\sigma_\varepsilon}\right)\frac{\partial \varepsilon}{\partial x_j}\right] + C_{1\varepsilon}\frac{\varepsilon}{k}(G_k + C_{3\varepsilon}G_b) - C_{2\varepsilon}\rho\frac{\varepsilon^2}{k} + S_\varepsilon \quad (5)$$

where σ_k is the Prandtl numbers for $k = 1.0$, G_k, generation of turbulent kinetic energy due to mean velocity gradients, G_b, generation of turbulent kinetic energy due to buoyancy, Y_M, contribution of the fluctuating dilatation in turbulence, σ_ε, Prandtl numbers for $\varepsilon = 1.3$, $C_{1\varepsilon} = 1.44$, $C_{2\varepsilon} = 1.92$, $C_{3\varepsilon} = 1.0$, and S_k, S_ε are user-defined source terms.

The equation for k is derived from the exact equation, whilst the equation for ε is obtained using physical reasoning and bears little resemblance to its mathematically exact counterpart.

Realizable k-ε model (Rl k-ε)

Shih et al.[23] developed the most-used Rl k-ε model. It was first developed based on the 'realizability' constraints; the positivity of normal Reynolds stresses and the Schwarz inequality for turbulent shear stresses. It was then found that the following flow types could be examined: (1) rotating homogeneous

shear flows, (2) boundary-free shear flows including a mixing layer, planar and round jets, (3) channel flow and flat plate boundary layers with and without a pressure gradient and (4) backward facing step separated flows. The turbulent kinetic energy equation for k is equation (4) whereas a new equation for ε, equation (6), has been derived from an exact equation for the transport of the mean-square vorticity fluctuation

$$\frac{\partial}{\partial t}(\rho\varepsilon)+\frac{\partial}{\partial x_j}(\rho\varepsilon u_j)=\frac{\partial}{\partial x_j}\left[\left(\mu+\frac{\mu_t}{\sigma_\varepsilon}\right)\frac{\partial\varepsilon}{\partial x_j}\right]+\rho C_1 S_\varepsilon-\rho C_2\frac{\varepsilon^2}{k+\sqrt{\upsilon\varepsilon}}+C_{1\varepsilon}\frac{\varepsilon}{k}C_{3\varepsilon}G_b+S_\varepsilon \quad (6)$$

where all parameters are the same as in the St k-ε model except for $\upsilon=$kinematic viscosity, $C_2=1.9$, $\sigma_\varepsilon=1.2$, $C_1=\max\ [0.43,\ \eta/(\eta+5)]$, $\eta=Sk/\varepsilon$, $S\equiv(2S_{ij}S_{ij})^{0.5}$, $S_{ij}=(\partial u_i/\partial x_j)+(\partial u_j/\partial x_i)$. The term of G_k is removed from the equation for ε, whilst the term of viscosity has been added because of the high effect from the Reynolds number in the flow.

Renormalization group k-ε model (RNG k-ε)

Yakhot and Orszag[24] derived the RNG k-ε turbulence model from the Navier–Stokes equations using a technique of renormalization group (RNG) methods. It significantly improved the accuracy for rapid flows. Because of the additional term in the ε equation R_ε the turbulence dissipation and mean shear can be better simulated at the interaction of phases. The effect of swirl on turbulence is included to enhance the accuracy for swirling flows. Due to a greater degree of non-linearity, computations with the RNG k-ε model tend to take 10–15% more CPU time than the St k-ε model. The equations for k and ε in the RNG k-ε turbulence are

$$\frac{\partial}{\partial t}(\rho k)+\frac{\partial}{\partial x_i}(\rho k u_i)=\frac{\partial}{\partial x_j}\left[\alpha_k\mu_{eff}\frac{\partial k}{\partial x_j}\right]+G_k+G_b-\rho\varepsilon-Y_M+S_k \quad (7)$$

$$\frac{\partial}{\partial t}(\rho\varepsilon)+\frac{\partial}{\partial x_i}(\rho\varepsilon u_i)=\frac{\partial}{\partial x_j}\left[\alpha_\varepsilon\mu_{eff}\frac{\partial\varepsilon}{\partial x_j}\right]+C_{1\varepsilon}\frac{\varepsilon}{k}(G_k+C_{3\varepsilon}G_b)-C_{2\varepsilon}\rho\frac{\varepsilon^2}{k}-R_\varepsilon+S_\varepsilon \quad (8)$$

where α_k, α_ε are inverse effective Prandtl numbers for k and ε, $\mu_{eff}=$effective viscosity$=\mu+\mu_t$, $C_{1\varepsilon}=1.42$, $C_{2\varepsilon}=1.68$, $C_{3\varepsilon}=1.0$. The term $R_\varepsilon=C_\mu\rho\eta^3(1-\eta/\eta_0)\varepsilon^2/k\left(1+\beta\eta^3\right)$ where $C_\mu=0.0845$, $\eta_0=4.38$, $\beta=0.012$.

Standard k-ω model (St k-ω)

The St k-ω model is based on the Wilcox k-ω model.[25] It was developed for working with the compressibility and shear flow spreading. It can predict free shear flow spreading rates that are in close agreement with measurements for wakes, mixing layers and plane, round and radial jets and is thus, applicable to wall-bounded flows and free shear flows. It is an empirical model based on the equations for k and ω, which can be the ratio of ε to k. They are

$$\frac{\partial}{\partial t}(\rho k)+\frac{\partial}{\partial x_i}(\rho k u_i)=\frac{\partial}{\partial x_j}\left[\Gamma_k\frac{\partial k}{\partial x_j}\right]+G_k-Y_k+S_k \quad (9)$$

$$\frac{\partial}{\partial t}(\rho\omega)+\frac{\partial}{\partial x_i}(\rho\omega u_i)=\frac{\partial}{\partial x_j}\left[\Gamma_\omega\frac{\partial\omega}{\partial x_j}\right]+G_\omega-Y_\omega+S_\omega \quad (10)$$

where G_ω is the generation of ω, Γ_k, Γ_ω, the effective diffusivity of k and ω, Y_k, the dissipation of k, Y_ω, the dissipation of ω due to turbulence, S_ω, the user-defined source term.

Shear stress transport k-ω model (SST k-)ω

Menter[26] developed the SST k-ω model to blend effectively the robust and accurate formulation of the k-ω model in the near-wall region with the free-stream independence of the k-ω model in the far field. The differences between the SST k-ω model and the standard model are: (1) the gradual change from the standard k-ω model in the inner region of the boundary layer, to a high-Reynolds-number version of the k-ε model in the outer part of the boundary layer and (2) the modified turbulent viscosity formulation to account for the transport effects of the principal turbulent shear stress. The equation for k is the same as in the St k-ω model (equation (9)), while the ω model can be shown as

$$\frac{\partial}{\partial t}(\rho\omega)+\frac{\partial}{\partial x_i}(\rho\omega u_i)=\frac{\partial}{\partial x_j}\left[\Gamma_\omega\frac{\partial\omega}{\partial x_j}\right]+G_\omega-Y_\omega+D_\omega+S_\omega \quad (11)$$

where D_ω represents the cross-diffusion term.

Results of velocity profile computations

Comparison between various turbulence models

Figure 2 shows a comparison example between the laboratory measurements and the model predictions with the five different turbulence algorithms. Overall, it is found that all turbulence models predict the velocity profiles rather well. The differences between the different models seem slightly accentuated near the free surface where air entrainment becomes significant.

The RMSE is a measure of the accuracy of a prediction in comparison to the measurements.

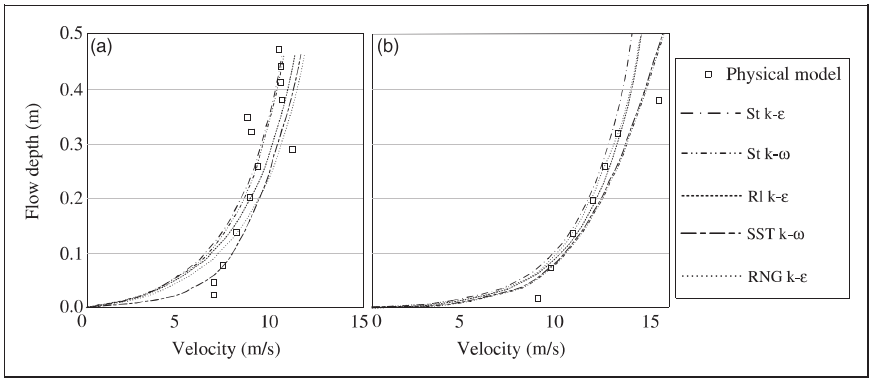

Figure 2. Comparison of the velocity profiles at a flow rate of 2.83 m^3/s at: (a) location B; (b) location E.

The RMSE is used to compare the results from physical and numerical velocity profiles. It is the square root of the average squared difference of the simulation results and the physical measurements as can be calculated using equation (12)

$$\mathrm{RMSE} = \sqrt{\frac{1}{m}\sum_{1}^{m}\left(Velocity_{physical} - Velocity_{numerical}\right)^2} \tag{12}$$

where m is the number of velocity measurements. The value of the RMSE is highly sensitive to large errors and low RMSE values reflect a high accuracy in the numerical prediction of the velocity profiles. The results at all locations show a good agreement with the physical data.

Considering the entire data set, the overall RMSE values calculated from the five turbulence models are summarized in Table 2. The lowest value of RMSE of 0.96 is found from using the Rl k-ε model. The highest value of RMSE of 1.07 is found from using the St k-ε model. The differences in RMSE values are not very significant but mean that the results from the St k-ε model are slightly less accurate than those of the Rl k-ε model.

For a more detailed comparison, the results of the RMSE at each vertical for all five turbulence models are compiled in Table 3. The location of maximum error is found at points D and E, which are located in the lower half of the stepped spillway. At point D the flow changed from the non-aerated zone to the aerated zone. Therefore, the changes in aerated conditions may largely affect the calculations and cause significant errors. In comparison with all five turbulence models, it was found that the Rl k-ε model is slightly better with an RMSE ranging from 0.19 to 1.82 m/s, which is very close to the RMSE from the RNG k-ε, St k-ω and SST k-ω models.

The turbulence model that gives the highest RMSE is the St k-ω model, which is developed from an empirical model. At all locations, most of the high RMSEs were observed 0.10 m above the pseudo-bottom.

Table 2. The overall RMSE values in meter per second.

Overall root mean square error, RMSE				
St k-ε	Rl k-ε	RNG k-ε	St k-ω	SST k-ω
1.07	0.96	1.03	1.05	1.00

Further development of the St k-ω model resulted in the SST k-ω model, which resulted in slightly more accurate results in the near-wall region, as shown in Figure 2.

The Rl k-ε model was developed for flows with a high Reynolds number. In the present study with Reynolds numbers between $1.68 \times 10^6 \leqslant Re \leqslant 7.21 \times 10^6$, the results of the Rl k-ε model were slightly better than those of the St k-ε model in the upper region. Due to the similar equations for both k and ε, the results from the RNG k-ε model are also similar to the St k-ε and the Rl k-ε models. However, with the additional term in the ε equation related to the main strain and turbulence quantities, the RNG k-ε model can be viewed as being slightly better.

Both k-ω models can also provide satisfactory results for near-wall treatments where the mesh is fine enough. In addition, it is more reliable for flows that have adverse pressure gradients. The results from using the SST k-ω model in the near-wall region in the present study show satisfactory agreement for fine mesh sizes. Thus, the point of interest is important in the selection of a turbulence model; e.g. the k-ω models are slightly preferable in the near-wall zone in the lower region, whilst the Rl k-ε model is preferable in the upper part of the velocity profile.

However, the turbulence models suggested by the previous studies in Table 1 by Chen et al.,[13] Cheng et al.[9] and Qian et al.,[14] are St k-ε, RNG k-ε, and Rl k-ε models, respectively. It can be seen that the newer developed turbulence model can be better used with the flow with higher flow rate. Moreover, Tongkratoke et al.[15] also found that Rl k-ε is the closest to the physical data compared with the other linear models. Most of flow rate in the cases simulated

Table 3. Detailed RMSE values at each location in meter per second.

Flow rate, Q (m^3/s)	location	Root mean square error, RMSE					Flow rate, Q (m^3/s)	location	Root mean square error, RMSE				
		St k-ε	RI k-ε	RNG k-ε	St k-ω	SST k-ω			St k-ε	RI k-ε	RNG k-ε	St k-ω	SST k-ω
1.6990	A	0.55	0.61	0.62	0.55	0.58	2.8317	A	1.08	0.67	1.03	1.09	1.03
	B	0.31	0.50	0.42	0.31	0.44		B	1.33	0.90	1.30	1.30	1.28
	C	0.50	0.47	0.48	0.50	0.49		C	0.24	0.19	0.19	0.18	0.18
	D	0.64	0.74	0.74	0.64	0.78		D	1.21	1.12	1.20	1.06	1.08
	E	0.75	0.74	0.67	0.75	0.68		E	1.64	1.02	1.63	1.59	1.59
2.2653	A	0.48	0.46	0.45	0.48	0.46	3.2848	A	0.61	0.48	0.48	0.61	0.45
	B	0.66	0.56	0.51	0.64	0.61		B	0.66	0.55	0.53	0.65	0.54
	C	0.73	0.69	0.69	0.71	0.69		C	NA	NA	NA	NA	NA
	D	1.05	0.97	0.97	0.97	0.91		D	1.57	1.48	1.53	1.52	1.34
	E	1.84	1.82	1.76	1.83	1.81		E	1.84	1.73	1.76	1.79	1.62
Minimum									0.24	0.19	0.19	0.18	0.18
Maximum									1.84	1.82	1.76	1.83	1.81

NA: No results from the physical data.

by Tongkratoke et al.[15] are close to or higher than the flow rate simulated by Qian et al.[14]

Changes in velocity profiles along the stepped spillway

The velocity profiles from all turbulence models tended to have the same shape, beginning with velocity gradually increasing from the pseudo-bottom until a maximum velocity was reached. The results of spillway overflow with the flow rate of $2.83\,m^3/s$ are shown in Figure 3(a). The velocity at the free surface gradually increases in the downstream direction. The lowest velocity at the free surface among all these measured locations is found at the upstream end. The velocity increases in the downstream direction and becomes relatively constant in the aerated zone. The numerical model with the RI k-ε turbulence model can simulate velocity profiles at all locations and it can easily be used to find the starting point of uniform flow. The results of spillway overflow near the downstream end with all flow discharges are shown in Figure 3(b). Considering different discharges, a higher discharge causes a higher flow depth but the flow velocity at the downstream end remains the same. Thus, the roughness of stepped spillways can be used to control the downstream velocity even when the inlet discharge is varied.

Previous studies described the dimensionless velocity distribution for skimming flow in terms of a power law, as shown in equation (13)

$$\frac{V}{V_{90}} = \left(\frac{y}{y_{90}}\right)^{\frac{1}{n}} \tag{13}$$

Different values of n were suggested from smaller scale experiments; Chanson and Toombes[27] found $n = 5.1$ and 6 for y_c/h of 1.5 and 1.1, respectively. Matos[28] found $n = 4$, whereas Chanson[18] suggested $n = 3.5$ and 4 for the earlier works of Frizell.[29] In the present study of skimming flow regimes, $n = 5.09$ is suggested under the limitation of the Reynolds number of $1.68 \times 10^6 \leqslant Re \leqslant 7.21 \times 10^6$. This number can be used to design the stepped spillway in various sizes. The designers or engineers can use this empirical formula to initially design the flow or even the flow depth that can be passed the stepped spillway. However, the numerical model, with the turbulence model suggested in the present study, is used to design more details of the stepped spillway.

Conclusions

CFD models are appropriate for the simulation of skimming flow velocity profiles on large stepped spillways. Five different turbulence models were tested against large-scale physical model experiments from Colorado State University, using a unit discharge as high as $2.69\,m^2/s$ and flow velocities of 15 m/s. The velocity profiles can be satisfactorily simulated by using the numerical model with five turbulence models: the Standard k-ε, the Realizable k-ε, the Renormalization group k-ε, the Standard k-ω and the Shear stress transport k-ω model. The differences in RMSE between the best and worst performance ranged from 0.96 to 1.07 and the profiles did not differ significantly. The k-ω models may be slightly better suited to the near-wall zone in the lower region of the velocity profile, whilst the RI k-ε model provided slightly better results in the upper part of the velocity profile. A reasonably good first approximation can be obtained with a power law for the velocity profile with $n = 5.09$. This analysis of velocity profiles on large stepped spillways nicely supplements the results of previous studies at a much smaller scale.

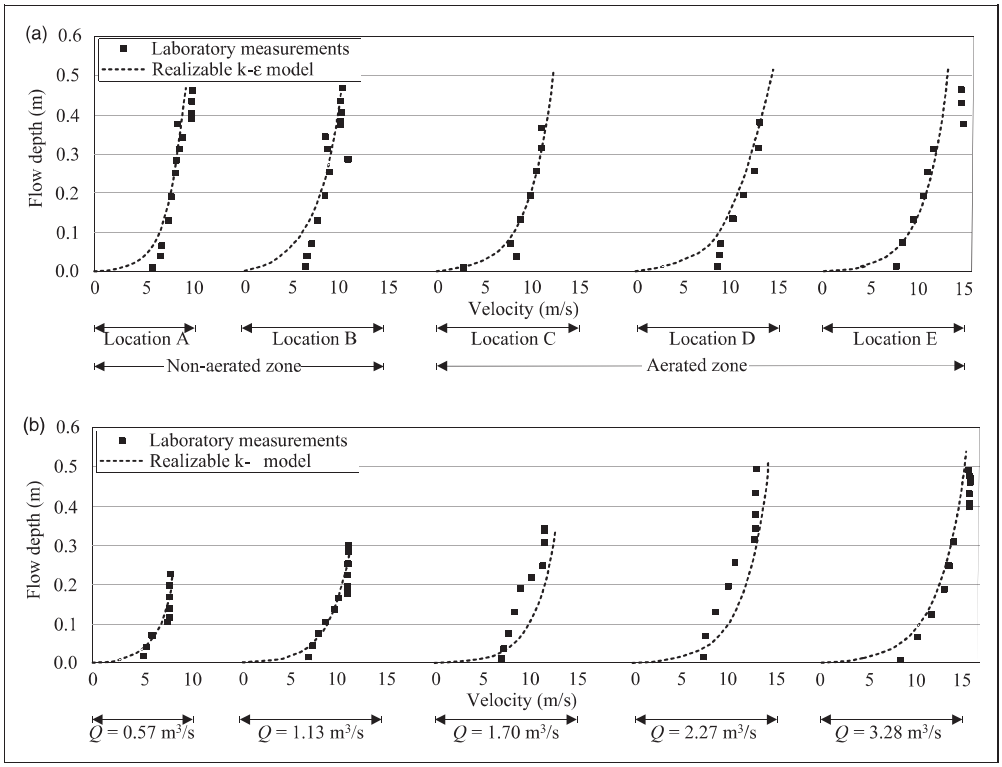

Figure 3. Flow velocity profiles along the stepped spillway: at a discharge of 2.83 m^3/s; (b) at the downstream end for different discharges.

Funding

The authors would like to thank the Thailand Research Fund/Royal Golden Jubilee PhD Grant (PHD/0225/2548 and BRG5280001) for financial support. Partial support from the National Research University Project of Thailand's Office of the Higher Education Commission is highly appreciated.

Acknowledgment

Sincere thanks to Professors James F Ruff and Robert N Meroney from Colorado State University for their supporting data, facilities and recommendations.

References

1. Boes RM and Hager WH. Hydraulic design of stepped spillways. *J Hydraul Eng-ASCE* 2003; 129: 671–679.
2. Felder S and Chanson H. Energy dissipation, flow resistance and gas-liquid interfacial area in skimming flows on moderate-slope stepped spillways. *Env Fluid Mech* 2009; 9: 427–441.
3. Chanson H. Prediction of the transition nappe/skimming flow on a stepped channel. *J Hydraul Res* 1996; 34: 421–429.
4. Chamani MR and Rajaratnam N. Onset of skimming flow on stepped spillways. *J Hydraul Eng-ASCE* 1999; 125: 969–971.
5. Chanson H, Yasuda Y and Ohtsu I. Flow resistance in skimming flows in stepped spillways and its modelling. *Can J Civil Eng* 2002; 29: 809–819.
6. Chanson H. *The hydraulics of stepped chutes and spillways*. Lisse: Balkema, 2002.
7. Boes RM and Hager WH. Two-phase flow characteristics of stepped spillways. *J Hydraul Eng-ASCE* 2003; 129: 661–670.
8. Ohtsu I, Yasuda Y and Takahashi M. Flow characteristics of skimming flows in stepped channels. *J Hydraul Eng-ASCE* 2004; 130: 860–869.
9. Cheng XJ, Chen YC and Luo L. Numerical simulation of air-water two-phase flow over stepped spillways. *Sci China Ser E* 2006; 49: 674–684.
10. Chanson H and Toombes L. Air–water flows down stepped chutes: turbulence and flow structure observations. *Int J Multiphas Flow* 2002; 28: 1737–1761.
11. Amador A. Characterization of the nonaerated flow region in a stepped spillway by PIV. *J Fluid Eng-ASME* 2006; 128: 1266–1273.
12. Kim SD, Lee HJ and An SD. Improvement of hydraulic stability for spillway using CFD model. *Int J Phys Sci* 2010; 5: 774–780.
13. Chen Q, Dai GQ and Liu HW. Volume of fluid model for turbulence numerical simulation of stepped spillway overflow. *J Hydraul Eng-ASCE* 2002; 128: 683–688.
14. Qian Z, Hu X, Huai W and Amador A. Numerical simulation and analysis of water flow over stepped spillways. *Sci China Ser E* 2009; 52: 1958–1965.
15. Tongkratoke A, Chinnarasri C, Pornprommin A, et al. Non-linear turbulence models for multiphase

recirculating free-surface flow over stepped spillways. *Int J Comput Fluid D* 2009; 23: 401–409.
16. Craft TJ, Launder BE and Suga K. Development and application of a cubic eddy-viscosity model of turbulence. *Int J Heat Fluid Fl* 1996; 17: 108–111.
17. Ward JP. *Hydraulic design of stepped spillways*. PhD Dissertation, Colorado State University, USA, 2002.
18. Chanson H. *Hydraulic design of stepped cascades, channels, weirs and spillways*. Oxford: Pergamon, 1995.
19. Hirt CW and Nichols BD. Volume of fluid for the dynamics of free boundaries. *J Comput Phys* 1981; 39: 201–225.
20. Erpicum S, Meile T, Dewals BJ, et al. 2D numerical flow modeling in a macro-rough channel. *Int J Numer Meth Fl* 2009; 61: 1227–1246.
21. Roache PJ. Quantification of uncertainty in computational fluid dynamics. *Annu Rev Fluid Mech* 1997; 29: 123–160.
22. Launder BE and Spalding DB. The numerical computation of turbulent flows. *Comput Method Appl M* 1974; 3: 269–289.
23. Shih TH, Liou WW, Shabbir A, et al. A new k-ε eddy viscosity model for high Reynolds number turbulent flows. *Comput Fluids* 1995; 24: 227–238.
24. Yakhot V and Orszag SA. Renormalization group analysis of turbulence: I. basic theory. *J Sci Comput* 1986; 1: 1–51.
25. Wilcox DC. Re-assessment of the scale-determining equation for advanced turbulence models. *AIAA J* 1988; 26: 1299–1310.
26. Menter FR. Zonal two equation k-ω turbulence models for aerodynamic flows. In: *24th Fluid Dynamics Conference*, Florida, USA, 6–9 July 1993, Paper No. AIAA 93-2906.
27. Chanson H and Toombes L. *Experimental investigations of air entrainment in transition and skimming flows down a stepped chute: application to embankment overflow stepped spillways*. Australia: Report, University of Queensland, 2001.
28. Matos J. Hydraulic design of stepped spillways over RCC dams. In: Minor HE and Hager WW (eds) *Proceedings of the International Workshop on Hydraulics of Stepped Spillways*, The Netherlands, 22–24 March 2000, pp.187–194.
29. Frizell KH. Hydraulics of stepped spillways for RCC dams and dam rehabilitations. In: *Proceedings of the 3rd Specialty Conference on Roller Compacted Concrete*, California, USA, 2–5 February 1992, pp.423–439.